

Selective CO₂ uptake in a bi-pillared layer 3D metal-organic framework of Zn(II)

Ritesh Haldar^a, Raghu Pradeep Narayan^b & Tapas Kumar Maji^{a, b, *}

Molecular Materials Laboratory, ^aNew Chemistry Unit and ^bChemistry and Physics of Materials Unit
Jawaharlal Nehru Centre for Advanced Scientific Research, Jakkur, Bangalore 560 064, India

Email: tmaji@jncasr.ac.in

Received 12 July 2012; revised & accepted 18 August 2012

A new two-fold interpenetrated 3D bi-pillared framework, {[Zn(1,4-bdc)(azbpy)]·DMF}_n (**1**), where 1,4-bdc = 1,4-benzene dicarboxylic acid, azbpy = 4,4'-azobipyridine and DMF = N,N-dimethyl formamide, has been synthesized from a mixed ligand system and characterized by single crystal as well as powder X-ray diffraction and thermogravimetric analysis. The metal center, Zn(II), having a trigonal bi-pyramidal geometry, is connected to the three different 1,4-bdc linkers in the equatorial positions while the axial positions are occupied by the two different 4,4'-azbpy pillars. The framework contains one-dimensional rectangular shaped channels along the *c* axis and the channel surfaces are decorated with the nitrogen atoms of -N=N- functional group from azbpy ligand. The desolvated framework has a specific surface area of ~ 40 m² g⁻¹ and shows excellent selective uptake of CO₂ at 195 K among other small gases like Ar, N₂ and H₂. (**1**) also adsorbs acetonitrile and benzene solvent vapors at 298 K.

Keywords: Metal organic frameworks, Selective CO₂ adsorption, Polar pore surface, Solvent vapour adsorption

Rapid extension of industrialization in modern era has caused a severe impact on the level of atmospheric CO₂ concentration. The current global climate change is partly associated with the increasing CO₂ concentration in the air. Carbon capture and sequestration from the flue gases is one approach to reduce atmospheric CO₂ concentration. Current conventional CO₂ capture technique involving chemisorption of CO₂ in amine solution is not an energy viable process. An alternative approach is reversible physisorption of CO₂ in porous materials. Among the various available porous materials, metal-organic frameworks (MOFs) or porous coordination polymers (PCPs) are most promising for the mentioned applications due to their regular and designable channel structure which is composed of strong and flexible coordination bonds.¹⁻⁵ The last couple of decades have witnessed extraordinary growth in the field of MOFs and many fascinating properties and applications have been unveiled including gas storage and separation,⁶⁻⁹ heterogeneous catalysis,¹⁰⁻¹² magnetism,¹³⁻¹⁵ sensing,¹⁶⁻²⁰ energy transfer²¹⁻²⁴ and drug delivery.²⁵⁻²⁶ The recognition and selective adsorption of gas molecules by MOFs are of paramount importance in concern to industry and environment. Earlier known conventional porous

materials like porous carbon,²⁷ and zeolites²⁸ have not been able to reach a satisfactory level of gas storage capacity and selectivity. Rather, new generation MOFs or PCPs are more capable to achieve the set goal. Here the basic building units are organic and inorganic moieties, and the framework structures can be easily modified to tune the adsorption properties in terms of storage capacity and selectivity.²⁹⁻³¹ Pore surface modified with the functional groups like -NH₂, -OH or hetero atoms (N, F, O) are promising candidates for CO₂ storage due to the specific Lewis acid-base interaction with the CO₂ molecule having large quadrupole moment.³²⁻³⁴ Additionally, the direct visualization of CO₂ molecules inside the pores have made the mechanistic pathways more clear and acceptable.³⁵⁻³⁶ Over the last few years different strategies has been adopted to make such materials and different functional groups have been incorporated in the pore surfaces to approach physically viable application; i.e., high amount of CO₂ uptake at low pressure and at ambient temperature.

In past few years, we have also come up with different newly designed frameworks for selective capture of CO₂.³⁷⁻³⁹ In continuation of this effort, herein we present a bi-pillared layer framework, {[Zn(1,4-bdc)(azbpy)]·DMF}_n (**1**), where 1,4-bdc =

1,4-benzene dicarboxylic acid, azbpy = 4,4'-azobipyridine and DMF = N,N-dimethyl formamide, having polar –N=N- functional groups on the pore surface. Bulk synthesis methodology and thermal stability of the framework have been studied. At 195 K, the desolvated framework shows excellent CO₂ selectivity among other gases like N₂, Ar and H₂. Furthermore, (1) also shows satisfactory uptake of acetonitrile and benzene vapors at 298 K.

Materials and Methods

All the reagents employed were commercially available and used as provided without further purification. Zinc nitrate [Zn(NO₃)₂·6H₂O] was obtained from Spectrochem and 1,4-bdc was obtained from Sigma Aldrich Co. 4,4'-Azobipyridine was synthesized following the reported literature procedure.⁴⁰

Elemental analysis was carried out using a Thermo Fischer Flash 2000 elemental analyzer. Infrared spectra were recorded on a Bruker IFS 66v/S FTIR spectrophotometer using KBr pellets in the region 4000–400 cm⁻¹. Powder X-ray diffraction (XRD) pattern of the product were recorded by using Cu-K radiation (Bruker D8 Discover; 40 kV, 30 mA). Thermogravimetric analysis (TGA) was carried out (Mettler Toledo) in nitrogen atmosphere (flow rate = 50 mL min⁻¹) in the temperature range 303 – 873 K (heating rate = 3 K min⁻¹).

Synthesis of {[Zn(1,4-bdc)(azbpy)]·DMF}_n (1)

A ligand solution in DMF (25 mL) was prepared by mixing of 1,4-bdc (1 mmol, 0.166 g) and azbpy (0.5 mmol, 0.092 g). A methanolic solution of zinc nitrate (1 mmol, 0.298 g) was prepared and layered on top of the ligand solution in a diffusion tube and left undisturbed. The orange colored block shaped crystals sticking on the sides of the tube were obtained after a couple of weeks. A good quality single crystal was separated and coated with paraffin oil and used for single crystal X-ray diffraction studies. Yield ~ 68 %. Anal. (%): Calcd. for C₂₀H₁₉ZnN₅O₅: C, 50.59; H, 4.01; N, 14.75. Found: C, 45.21; H, 5.01; N, 7.49; Observed: C, 50.59; H, 4.01; N, 14.75. Found: C, 45.11; H, 5.41; N, 7.41%. FT-IR (KBr pellet, cm⁻¹): 3456, 1593, 1555, 1378, 1410, 1214, 1028, 995.

X-ray crystallography

Single crystal X-ray structural data of (1) was collected on a Bruker Smart-CCD diffractometer equipped with a normal focus, 2.4 kW sealed tube X-ray source with graphite monochromated Mo-K α

radiation ($\lambda = 0.71073 \text{ \AA}$) operating at 50 kV and 30 mA. The program SAINT⁴¹ was used for integration of diffraction profiles. Absorption correction was made with SADABS⁴² program. The structure was solved by SIR 92⁴³ and refined by full matrix least square method using SHELXL-97.⁴⁴ All the hydrogen atoms were fixed by HFIX and placed in ideal positions. Potential solvent accessible area or void space was calculated using the PLATON multipurpose crystallographic software.⁴⁵ All crystallographic and structure refinement data of (1) is summarized in Table 1. All calculations were carried out using SHELXL 97, PLATON and WinGX system, ver 1.70.01.⁴⁶

Adsorption studies

The adsorption isotherms of N₂ (77 K and 195 K), CO₂ (195 K), Ar (195 K) and H₂ (195 K) for compound (1) were measured by using a Quantachrome Quadrasorb SI analyzer. The adsorbent sample (100–150 mg) was placed in the sample chamber (of about 17.5 mL) maintained at $T = 433 \pm 0.03 \text{ K}$ under a 0.1 Pa vacuum for about 6 h prior to measurement of the isotherm. Helium gas at a certain pressure was introduced in the gas chamber and allowed to diffuse into the sample chamber by opening the valve. The change in pressure allowed an accurate determination of the volume of the total gas phase. The amount of gas adsorbed was calculated

Table 1—Crystal data and structure refinement parameters of compound (1)

Parameters	(1)
Emp. formula	C ₂₁ H ₁₈ N ₅ O ₅ Zn
Mol. wt.	485.79
Crystal system	Monoclinic
Space group	<i>P</i> 2 ₁ / <i>n</i> (No. 14)
<i>a</i> (Å)	11.5888(5)
<i>b</i> (Å)	15.4052(6)
<i>c</i> (Å)	12.2398(5)
<i>V</i> (Å ³)	2029.30(15)
<i>Z</i>	4
<i>T</i> (K)	293
λ (Mo-K α)	0.71073
<i>D_c</i> (g cm ⁻³)	1.590
μ (mm ⁻¹)	1.256
θ_{max} (deg.)	32.0
Total data	23767
Unique reflection	6735
<i>R</i> _{int}	0.069
[<i>I</i> > 2 σ (<i>I</i>)]	4239
<i>R</i> ^a	0.0926
<i>R</i> _w ^b	0.2767
GOF	1.03

readily from pressure difference ($P_{cal} - P_e$), where P_{cal} is the calculated pressure with no guest adsorption and P_e is the observed equilibrium pressure. High pressure CO₂ adsorption measurement at 298 K was carried out on a fully computer controlled volumetric high pressure instrument (Belsorp-HP, BEL Japan). CO₂ gas used for the measurement was of 99.999 % purity. For the measurements, approximately 300 mg of sample was taken in a stainless-steel sample holder and degassed at 433 K for a period of 12 h under 0.1 Pa vacuum. Dead volume of the sample cell was measured with He gas of 99.999 % purity. Non-ideal correction for CO₂ gas was made by applying virial coefficients at 298 K.

The adsorption of different solvents like benzene (C₆H₆) and acetonitrile (CH₃CN) at 298 K was measured in the vapor state by using Belsorp-aqua-3 analyzer. Prior to measurements, the sample was treated at 433 K for about 10 h under vacuum. The different solvent molecules used to generate the vapor were degassed fully by repeated evacuation. Dead volume was measured with helium gas. The adsorbate was placed into the sample tube and the change of the pressure was monitored. The degree of adsorption was determined by the decrease in pressure at the equilibrium state. All operations were computer controlled and automatic.

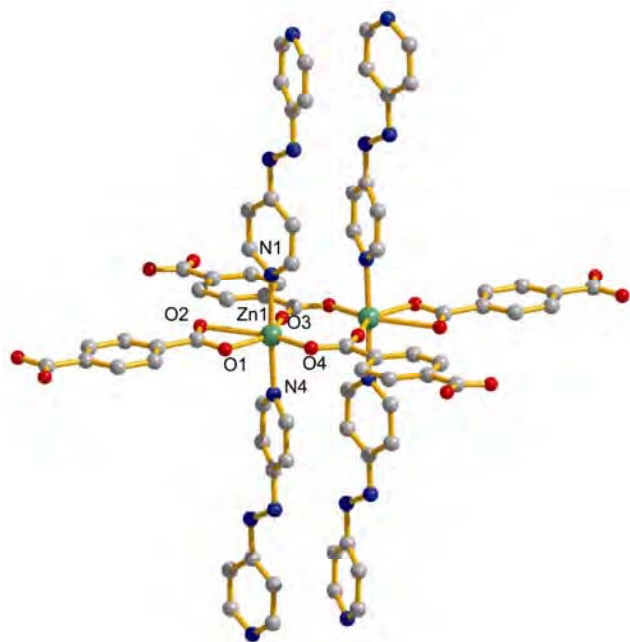


Fig. 1—Coordination environment of Zn(II) metal center in compound (1).

Results and Discussion

Crystal structure of {[Zn(1,4-bdc)(azbpy)]·DMF}_n (1)

Compound (1) crystallizes in monoclinic $P2_1/n$ space group. X-ray structure determination shows a 3D coordination framework of Zn(II) bridged by the 1,4-bdc and 4,4'-azbpy linkers. Each Zn(II) is connected to the three different oxygen atoms from the three different 1,4-bdc linkers in the equatorial positions and the axial positions are occupied by the two nitrogen atoms (N1, N2) from the two different 4,4'-azbpy pillars (Fig. 1). Therefore, each Zn(II) is in trigonal bi-pyramidal geometry with ZnO₃N₂ chromospheres. Zn1-O and Zn1-N bond distances are in the range of 2.026(3) – 2.048(3) Å and 2.165(4) – 2.189(4) Å, respectively. The distortion from the perfect TBP geometry is reflected in the *cisoid* angles (Table 2). Two 1,4-bdc connect two Zn(II) centers in a syn-syn fashion forming Zn₂(CO₂)₂ SBU and this binuclear core is connected by another two 1,4-bdc by monodentate carboxylate oxygen atoms forming a perfectly 2D planar [Zn₂(1,4-bdc)₂]_n sheet lying in the crystallographic *bc* plane (Fig. 2a). Each 2D sheet is further pillared by the 4,4'-azbpy forming a 3D pillared layer framework (Fig. 2b). It is worth mentioning that the two Zn(II) centers of the binuclear core in the 2D sheet are connected by the 4,4'-azbpy forming bi-pillared layer-type framework. These nets are again two-fold interpenetrated reducing the available void space in the framework. However, along the crystallographic *b* axis the framework shows rectangular shaped channels⁴⁷ (2.21 Å × 4.15 Å), which are occupied by guest DMF molecules and there is no additional opening along *c* and *a* axis (Fig. 3). Topological analysis by TOPOS 4.0⁴⁸ suggests formation of a (2, 3, 5)-connected net

Table 2—Selected bond lengths (Å) and angles (°) for (1)

Bond lengths			
Zn1-O1	2.004(5)	Zn1-O2	2.566(6)
Zn1-O3	2.004(5)	Zn1-O4	2.035(6)
Zn1-N1	2.209(4)	Zn1-N4_a	2.194(4)
Bond angles			
O1-Zn1-O2	52.35(17)	O1-Zn1-O3	97.38(19)
O1-Zn1-O4	137.18(19)	O1-Zn1-N1	94.69(16)
O1-Zn1-N4_a	89.66(16)	O2-Zn1-O3	149.28(17)
O2-Zn1-O4	85.27(17)	O2-Zn1-N1	86.97(16)
O2-Zn1-N4_a	94.38(15)	O3-Zn1-O4	125.34(19)
O3-Zn1-N1	91.11(17)	O3-Zn1-N4_a	90.00(16)
O4-Zn1-N1	88.02(16)	O4-Zn1-N4_a	87.64(16)
N1-Zn1-N4_a	175.34(12)		

with Schläfli symbol $\{4.8^2\}\{4.8^8.12\}\{8\}$ (Fig. 4). Removal of guest molecules creates a void space of $\sim 24\%$ ($\sim 492 \text{ \AA}^3$) of the total cell volume as calculated by PLATON. The distances between Zn(II)...Zn(II) centers connected by 1,4-bdc and azbpy linkers are 11.084 \AA and 13.375 \AA , respectively.

Thermal stability

TG analysis of compound **1** (Fig. 5) carried out under nitrogen atmosphere shows a weight loss of 25% (calc. wt. loss $\sim 24.9\%$) in the range $303 - 448 \text{ K}$, corresponding to one DMF guest molecule. The

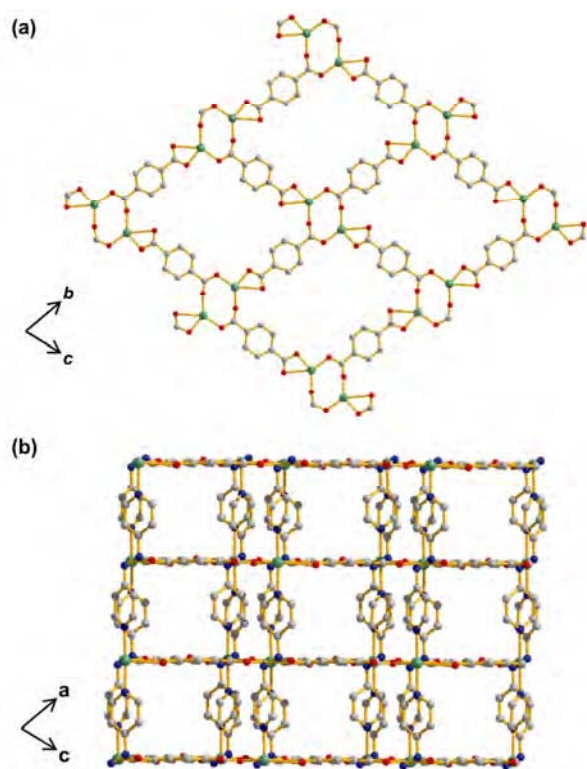


Fig. 2—(a) 2D sheet of compound (**1**) along bc plane, (b) 3D bi-pillared layer structure along b direction, and, (c) rectangular channels along b direction.

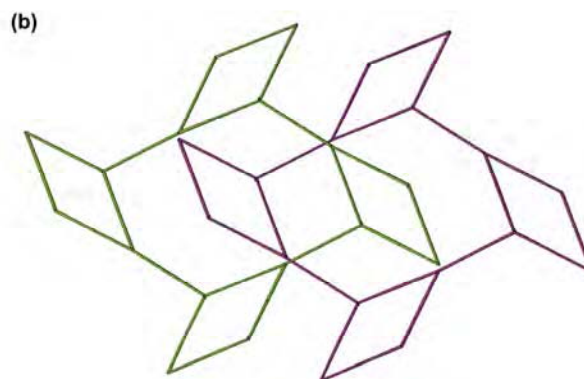
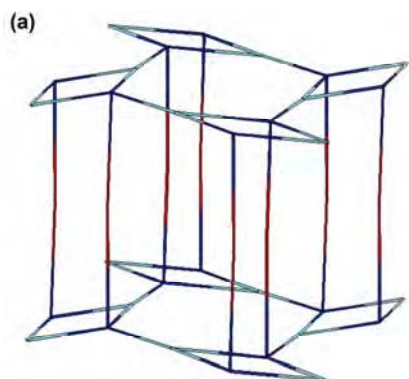


Fig. 4—(a) 2, 3, 5-Connected net of compound (**1**), and, (b) view of interpenetrated nets.

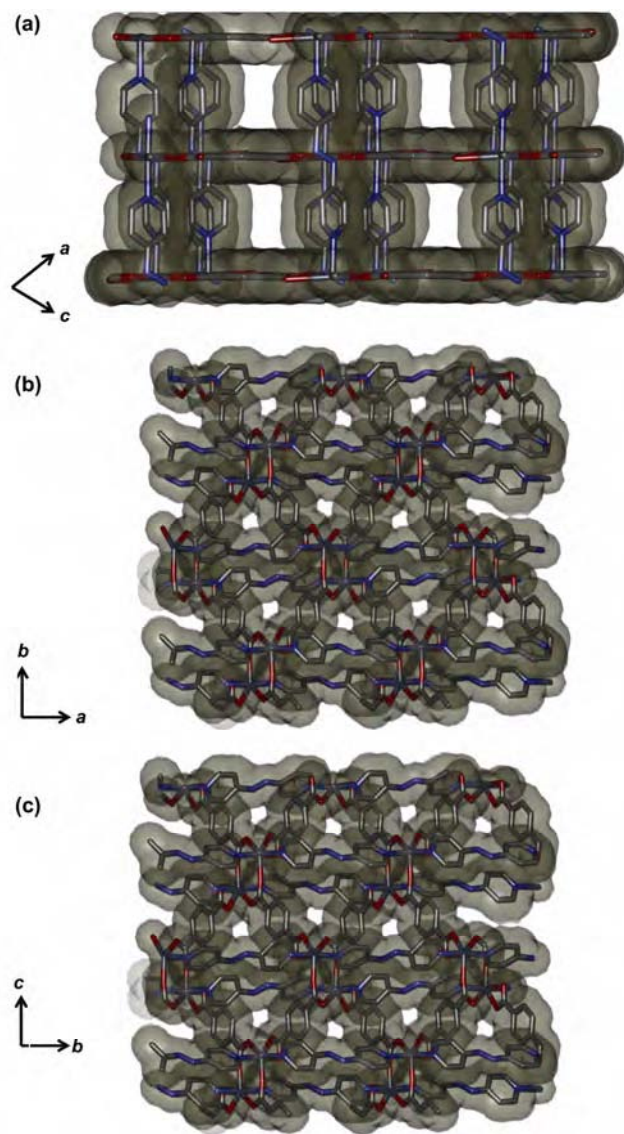


Fig. 3—View of surface added pores along different directions. [(a) along b axis; (b) along c axis; (c) along a axis].

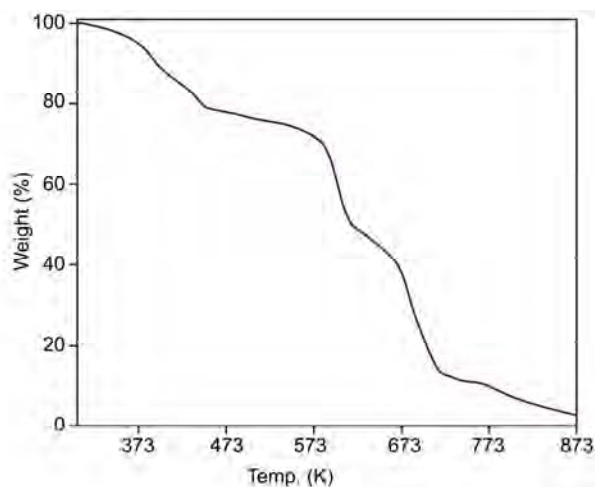


Fig. 5—TGA curve for compound (**1**) under N₂ atmosphere in the temperature range of 30–600 °C.

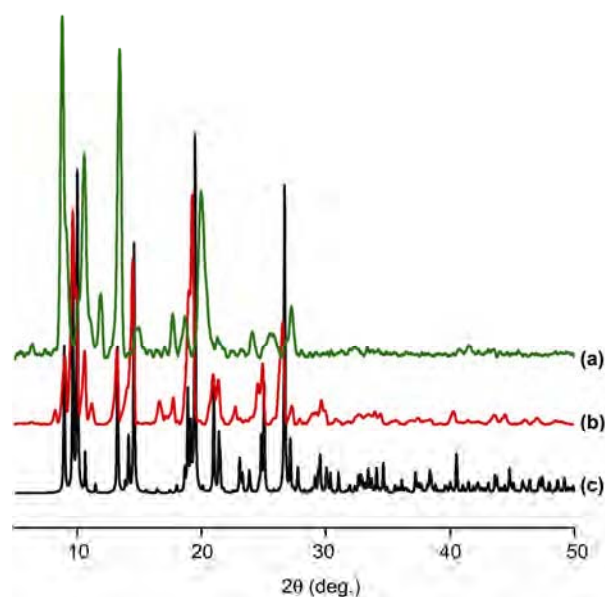


Fig. 6—The PXRD patterns of compound (**1**). [(a) simulated; (b) as-synthesized; (c) heated at 433 K].

dehydrated framework, $\{Zn(1,4\text{-}bdc)(azbpy)\}_n$ (**1'**) is stable up to ~ 573 K. Upon further heating, compound (**1**) decomposed to an unidentified product. After removal of guest solvent molecules from (**1**), there was appearance of some new peaks at $2\theta = 11.95^\circ$ and 15.045° and shifting of the peak at $2\theta = 25.615^\circ$, indicating structural change (Fig. 6). Removal of solvent molecules creates a void space, and hence, motion of the interpenetrated nets is the most probable reason of such a structural change.

Selective CO₂ adsorption

Encouraged by high thermal stability and available void space of the compound (**1**) after removal of guest

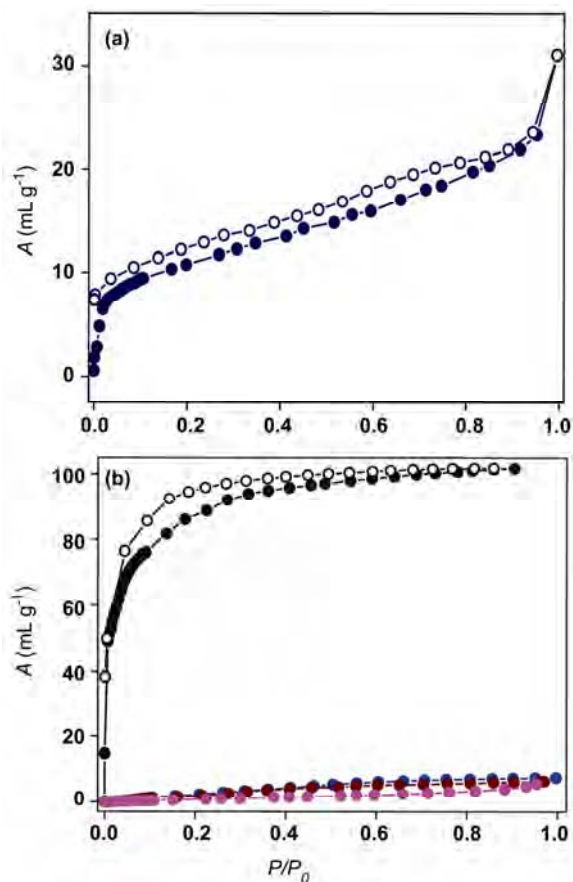


Fig. 7—(a) N₂ adsorption isotherm of (**1'**) at 77 K, and (b) CO₂ (black), N₂ (blue), H₂ (pink) and Ar (wine) gas adsorption isotherms at 195 K. [Adsorption: filled circles; Desorption: open circles].

solvent molecules, we carried out the adsorption studies with different gases and solvent vapours. At 77 K, desolvated (**1**) (i.e., **1'**) showed a very small uptake of N₂ (kinetic diameter ~ 3.64 Å)⁴⁹ with type-II profile. The corresponding BET surface area of **1'** was ~ 40 m²/g (Fig. 7a). The one-dimensional channel system in the framework and the comparable pore size to the kinetic diameter of N₂ result in high diffusion barrier of N₂ at 77 K. However, surprisingly we observed a low pressure uptake of CO₂ with typical type-I profile, indicating the microporous nature of the framework. The framework uptakes ~ 102 mL/g at $P/P_0 \sim 1$ which corresponds to 20 wt% of CO₂ storage capacity. The desorption path does not follow the adsorption path completely and shows a small hysteresis. At 195 K, compound (**1'**) exhibits negligible uptake of H₂, Ar and N₂ (Fig. 7b) suggesting high CO₂ selectivity in the framework. Such selectivity can be attributed to the specific host-guest interaction between CO₂ and framework as the

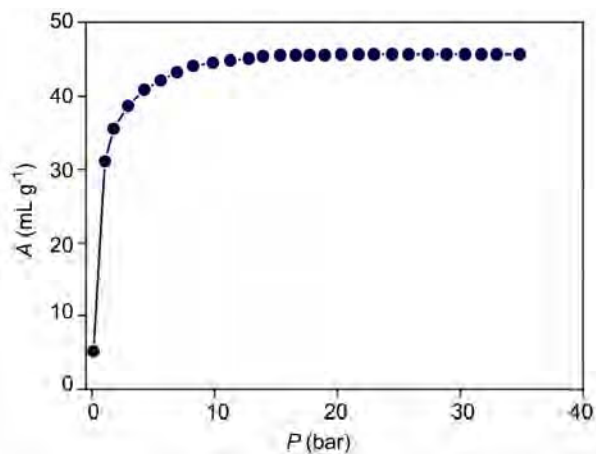


Fig. 8—CO₂ adsorption profile at 298 K up to 40 bar pressure.

former has high quadrupole moment and the latter has polar nature of the pore surface. The channel apertures are decorated with $-N=N-$ groups (from 4,4'-azbpy) and $Zn_2(COO)_2$ SBU and these moieties act as efficient adsorption sites to interact with CO₂. High interaction between pore surface and adsorbent is realized by high heat of adsorption, ~ 32.1 kJ/mol, calculated using DR equation.⁵⁰ Importantly, at 298 K, (**1'**) can adsorb ~ 9 wt% of CO₂ at 30 bar pressure with a typical type-I profile (Fig. 8). It has been observed that MOFs synthesized from ligands having pendant heteroatom centers or polar functional groups can create polar pore surface and this eases the higher CO₂ uptake. The recent works reported by our group show that presence of heteroatom centers (N) and the different functional groups in the linker can modulate the CO₂ uptake significantly.³⁷⁻³⁹ Though CO₂ uptake is mostly a cooperative phenomenon, strong interaction with the pore surface induces strong binding, and hence, high heat of adsorption can be realized. In some instances we observed that though the pore size is not enough (smaller than the kinetic diameter of CO₂, 3.3 Å), CO₂ can diffuse through the pores because of the interaction with the host framework based on structural transformation.⁴⁹ These cases are not common and are observed for CO₂ adsorption only. It is the high quadrupole moment of the CO₂ that leads to such a kind of dynamic behaviour in the framework.

To prove further the polar nature of the pore surface, we have studied the solvent vapour adsorption of benzene and acetonitrile at 298 K. Benzene solvent vapour adsorption profile shows a typical type-I curve and the saturation amount is 40 mL at $P/P_0 \sim 0.9$, which corresponds to ~ 0.75 benzene

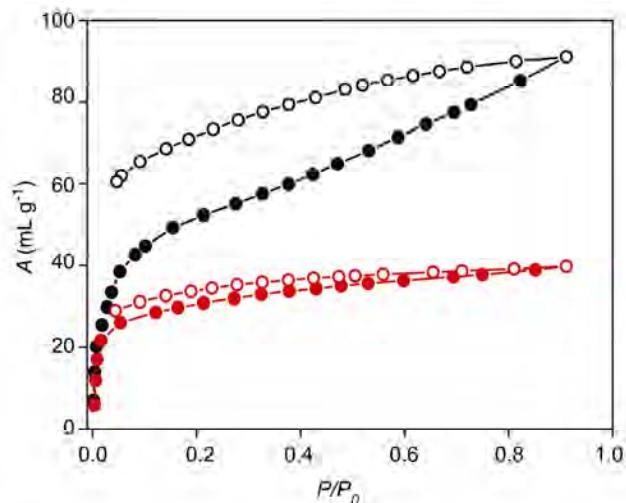


Fig. 9—Benzene (red) and acetonitrile (black) solvent vapour adsorption profiles of (**1'**) at 298 K. [Adsorption: filled circles, Desorption: open circles].

molecules per formula (Fig. 9). A slightly different adsorption profile was obtained with acetonitrile vapour. A steep uptake was observed at the low pressure region. Beyond $P/P_0 \sim 0.32$, the uptake amount of acetonitrile increased gradually with any further increase pressure, to finally 91 mL/g at P/P_0 0.91 corresponding to ~ 1.7 molecules per formula (Fig. 9). The hysteretic sorption profile as observed by the non-coincidence of the desorption profile with the adsorption profile, unlike benzene sorption profile, and non-release of all the adsorbed molecules (~ 1 acetonitrile per formula) indicates strong host-guest interaction between pore surface of (**1**) and acetonitrile. This result further corroborates the highly polar nature of the compound (**1**).

Conclusions

In conclusion, we have synthesized a new two-fold interpenetrated bi-pillared layer framework, $\{[Zn(1,4\text{-bdc})(\text{azbpy})]\cdot\text{DMF}\}_n$ (**1**) from a mixed ligand system of 1,4-bdc and azbpy. The desolvated framework (**1'**) is thermally stable, which can be corroborated to the rigid oxo-bridged $Zn_2(COO)_2$ unit and interpenetration of the framework. At 195 K, (**1'**) shows excellent selectivity for CO₂ gas among other gases like N₂, H₂ and Ar. The selectivity can be attributed to the strong interaction between the polar pore surface of the framework and CO₂ molecules. The polarity of the framework is further evidenced by solvent vapour studies. Our results demonstrate that by modifying the functional groups of the organic

linkers, it is possible to design and synthesize CO₂ selective porous MOFs, which may have potential application in CO₂ sequestration.

Supplementary Data

Crystallographic data of compound (1) reported herein have been deposited with the Cambridge Crystallographic Data Centre under CCDC No. 884553. Copies of the data can be obtained free of charge, on application to CCDC, 12 Union Road, Cambridge, CB2 1 EZ, UK. (Fax: +44- (0) 1223-336033; Email: deposit@ccdc.cam.ac.uk).

References

- 1 Ferey G, *Chem Soc Rev*, 37 (2008) 191.
- 2 Kitagawa S, Kitaura R & Noro S-I, *Angew Chem, Int Edn*, 43 (2004) 2334.
- 3 Perry IV J J, Perman J A & Zaworotko M J, *Chem Soc Rev*, 38 (2009) 1400.
- 4 Long J R & Yaghi O M, *Chem Soc Rev*, 38 (2009) 1213.
- 5 Spokoyny A M, Kim D, Sumrein A & Mirkin C A, *Chem Soc Rev*, 38 (2009) 1218.
- 6 Kosal M E, Chou J-H, Wilson S R & Suslick K S, *Nat Mater*, 1 (2002) 118.
- 7 Li H, Eddaoudi M, O'Keeffe M & Yaghi O M, *Nature*, 402 (1999) 276.
- 8 Kondo M, Okubo T, Asami A, Noro S I, Yoshitomi T, Kitagawa S, Ishii T, Matsuzaka H & Seki K, *Angew Chem, Int Edn*, 38 (1999) 140.
- 9 Kanoo P, Matsuda R, Higuchi M, Kitagawa S & Maji T K, *Chem Mater*, 21 (2009) 5860.
- 10 Ma L, Abney C & Lin W, *Chem Soc Rev*, 38 (2009) 1248.
- 11 Lee J Y, Farha O K, Roberts J, Scheidt K A, Nguyen S T & Hupp J T, *Chem Soc Rev*, 38 (2009) 1450.
- 12 Horike S, Dincă M, Tamaki K & Long J R, *J Am Chem Soc*, 130 (2008) 5854.
- 13 Kanoo P, Madhu C, Mostafa G & Maji T K, *Dalton Trans*, (2009) 5062.
- 14 Maji T K, Kaneko W, Ohba M, Kitagawa S, *Chem Commun*, (2005) 4613.
- 15 Kurmoo M, *Chem Soc Rev*, 38 (2009) 1353.
- 16 Cui Y, Yue Y, Qian G & Chen B, *Chem Soc Rev*, 112 (2012) 1126.
- 17 Chen B, Wang L, Zapata F, Qian G & Lobkovsky E B, *J Am Chem Soc*, 130 (2008) 6718.
- 18 Kreno L E, Leong K, Farha O K, Allendorf M, Duyne R P V & Hupp J T, *Chem Soc Rev*, 112 (2012) 1105.
- 19 Kanoo P, Ghosh A C, Cyriac S T & Maji T K, *Chem Eur J*, 18 (2012) 237.
- 20 Rocha J, Carlos L D, Paz F A A & Ananias D, *Chem Soc Rev*, 40 (2011) 926.
- 21 Lee C Y, Farha O K, Hong B J, Sarjeant A A, Nguyen S T & Hupp J T, *J Am Chem Soc*, 133 (2011) 15858.
- 22 Kent C A, Mehl B P, Ma L, Papanikolas J M, Meyer T J & Lin W, *J Am Chem Soc*, 132 (2010) 12676.
- 23 Matthes P R, Höller C J, Mai M, Heck J, Sedlmaier S J, Schmiechen S, Feldmann C, Schnick W & Müller-Buschbaum K, *J Mater Chem*, 22 (2012) 10179.
- 24 Mohapatra S, Adhikari S, Rijju H & Maji T K, *Inorg Chem*, 51 (2012) 4891.
- 25 Horcajada P, Serre C, Sebban M, Taulelle F & Férey G, *Angew Chem, Int Ed*, 45 (2006) 5974.
- 26 Horcajada P, Serre C, Maurin G, Ramsahye N A, Balas F, Vallet-Regi M, Sebban M, Taulelle F & Férey G, *J Am Chem Soc*, 130 (2008) 6774.
- 27 Choi S, Drese J H & Jones C W, *ChemSusChem*, 2 (2009) 796.
- 28 Zukal A, Dominguez I, Mayerová J & Cezka J, *Langmuir*, 25 (2009) 10314.
- 29 Kanoo P, Sambhu R & Maji T K, *Inorg Chem*, 50 (2011) 400.
- 30 Horike S, Kishida K, Watanabe Y, Inubushi Y, Umeyama D, Sugimoto M, Fukushima T, Inukai M & Kiatagaw S, *J Am Chem Soc*, 134 (2012) 9852.
- 31 Colombo V, Montoro C, Maspero A, Palmisano G, Masciocchi N, Galli S, Barea E & Navarro J A R, *J Am Chem Soc*, (2012) 10 1021/ja305267m.
- 32 Vaidhyanathan R, Iremonger S S, Dawson K W & Shimizu G K H, *Chem Commun*, 35 (2009) 5230.
- 33 Mallick A, Saha S, Pachfule P, Roy S & Banerjee R, *Chem Commun*, 20 (2010) 9073.
- 34 Arstad R, Blom R & Swang O, *J Phys Chem A*, 111 (2007) 1222.
- 35 Vaidhyanathan R, Iremonger S S, Shimizu G K H, Boyd P G, Alavi S & Woo T K, *Science*, 330 (2010) 650.
- 36 Maji T K, Mostafa G, Matsuda R & Kitagawa S, *J Am Chem Soc*, 127 (2005) 17152.
- 37 Haldar R & Maji T K, *CrystEngComm*, 14 (2012) 684.
- 38 Dey R, Haldar R, Maji T K & Ghoshal D, *Cryst Growth Des*, 11 (2011) 3905.
- 39 Nagaraja C M, Haldar R, Maji T K & Rao C N R, *Cryst Growth Des*, 12 (2012) 975.
- 40 Brown E V & Granneman G R, *J Am Chem Soc*, 97 (1975) 621.
- 41 SMART (ver 5 628), SAINT (ver 6 45a), XPREP, SHELXTL, (Bruker AXS Inc Madison, Wisconsin, USA) 2004.
- 42 Sheldrick, G M, *Siemens Area Detector Absorption Correction Program*, (University of Göttingen, Göttingen, Germany) 1994.
- 43 Altomare A, Cascarano G, Giacovazzo C & Gualaradi A, *J Appl Cryst*, 26 (1993) 343.
- 44 Sheldrick G M, *SHELXL-97, Program for Crystal Structure Solution and Refinement*, (University of Göttingen, Göttingen, Germany) 1997.
- 45 Spek A L, *J Appl Crystallogr*, 36 (2003) 7.
- 46 Farrugia L J, *WinGX-A Windows Program for Crystal Structure Analysis*, *J Appl Cryst*, 32 (1999) 837.
- 47 The sizes of the channels were calculated considering the van der Waals radii of the atoms.
- 48 Spek A L, *J Appl Cryst*, 36 (2003) 7.
- 49 Webster C E, Drago, R S & Zerner, M C, *J Am Chem Soc*, 120 (1998) 5509.
- 50 Dubinin M M, *Chem Rev*, 60 (1960) 235.